A BLE-Based Marathon Runner Timing System Using Multi-Directional Antennas to Improve Timing Stability

Huang-Chen Lee, *Senior member, IEEE*, Soun-Cheng Wang, and Yu-Kai Chen

Abstract—Marathons have recently become popular sporting activities. Due to the competitive nature of marathons, organizers often use automatic timing systems to ensure fairness and impartiality. However, for small- and medium-sized marathon organizers, the existing timing systems are too costly to deploy, so human supervision and timing are still often used. This study proposes an automatic timing system for marathons based on Bluetooth-Low-Energy (BLE) with multiple antennas. Compared to similar studies, this design has higher timing stability. By comparing the characteristics of the received signal strength (RSS) received from multiple antennas, our system can determine when the runner passes the checkpoint. This study uses deep learning algorithms to deal with noisy RSS from multiple antennas. During the evaluation, 20 runners participated in experiments at four locations, demonstrating the scalability of the proposed system. The results showed that the accurate detection of the timing for marathon runners was 96.8%, which could be further increased to 100% if a one-second timing error is acceptable.

***Index Terms*—Marathon runner, multiantenna, directional antenna, Bluetooth Low Energy, embedded system, RFID.**

I. Introduction

A marathon is a long-distance road running race. It is particularly important to track whether a runner has passed the checkpoints, the time at which they pass the checkpoints, and the time at which they complete the entire race. Before timing systems became popular in marathon races, timekeepers would manually determine whether a runner had passed the finish line with the assistance of high-speed scanning cameras taking continuous photos. This approach consumed a considerable amount of manpower, required the use of costly high-speed cameras, and led to frequent timing errors. In addition, for runners and spectators, the process and results of the race are less transparent and more prone to disputes.

In order to ensure the impartiality of the race, automatic timing systems are often used to automatically identify and record the presence of runners, including when they start, pass the checkpoint, and reach the finish line. Currently, radio frequency identification (RFID) [1][2][3] timing systems are the most widely used to accurately time runners. As shown in Fig. 1(a), an RFID tag is battery-free and inexpensive. The runner wears the RFID tag on their feet, and it is detected by the RFID reader mat when the runner passes the checkpoint. Meanwhile, the RFID's short communication range, usually less than 10 cm, ensures the precise detection of the RFID tag when the runner is passing the checkpoint. Although RFID timing system have already been used widely and proven to be useful in timing runners, their major drawback is that the checkpoint's hardware is bulky and expensive, which prohibits the use of this type of system in small- and medium-sized marathons. Also, the reader may fail to detect the runner if they are not close enough to the RFID reader mat, resulting in the loss of their timing information.

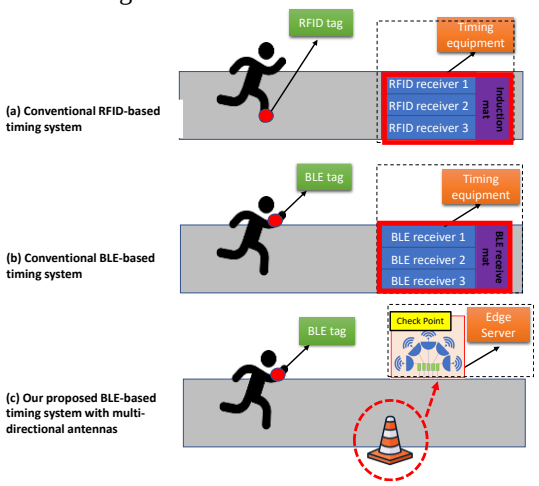

Fig. 1 (a) Conventional RFID-based timing system, (b) conventional BLE-based timing system, and (c) the proposed BLE-based timing system with multidirectional antennas.

Recently, several new designs have exploited the use of Bluetooth-Low-Energy (BLE) [14] to replace RFID. BLE-based timing systems [4][5], as shown in Fig. 1(b), also use extremely low energy and perform short-distance communication in the range of several meters. The design of a BLE tag allows it to broadcast a BLE advertisement to the BLE receiver. Runners wearing BLE tags are detected by nearby BLE receivers. The runner passing the receiver is detected according to the change of received signal strength (RSS). This approach has been used widely [6][7][8] in positioning applications. Checkpoints often have multiple BLE receivers installed to increase the chance of receiving BLE tag advertisements. Therefore, BLE can replace RFID as an automatic timekeeper. This type of timing system is affordable for small- and medium-sized marathons.

Although several similar designs using BLE have been proposed, they are often inferior due to the nature of wireless signals, resulting in the failed detection of a runner or the false detection of a runner who is far in distance or even off-route. The main reason is that radio waves have characteristics such as scattering and diffraction, which are greatly affected by the environment at the site. Therefore, it is rare to see BLE timing systems in real marathon events because of their unreliability.

In order to respond to the desperate need for a better

automatic marathon timing system, this study proposes a new BLE-based system that features multiple directional antennas for the BLE receivers in the checkpoint to collect more characteristics of BLE advertisement broadcasted from the runner's BLE tag, as shown in Fig. 1(c). Directional antennas have a higher signal gain in their designated direction and can provide more hints to determine the tag's location and distance. This method can avoid relying solely on the single omnidirectional signal antenna of the BLE receiver to receive the wireless signal of the tag, making it difficult to determine whether the tag advertisement represents the passage of a runner. We will explain the issue of the existing BLE timing system in the following chapters.

In the proposed design, the BLE receivers collect the BLE advertisement from multiple directional antennas and then use deep learning algorithms to determine the runner's current behavior (i.e., running pass to the checkpoint or just wandering back and forth near the checkpoint). The proposed design can reduce errors and even provide anti-cheating features to prevent malicious behaviors (e.g., taking detours and shortcuts). The proposed design has been confirmed to lower the miss and false positive rate and raise the hit rate of detecting runners.

In summary, the goals of this study are listed as follows:

- The proposed system must be able to detect the runner passing the checkpoint reliably.
- The system must be able to detect abnormal behaviors of marathon runners.
- This system must be lightweight and easy to install to incentivize marathon organizers to use it.
- Multiple runners passing the checkpoint should not affect the accuracy of detection.

II. Related works

The advent of RFID technology has made it possible to fully automate marathon timing to improve the fairness of the race and to reduce the number of timekeepers. This allows us to display the time of runners passing by each checkpoint in real time, making the results of the whole race more convincing. As far as we know, the World Athletics Federation [6] has defined the specifications for timing systems for sprinting, but not for marathons. By surveying the marathon timing products [13] on the market and referring to the historical records of marathons [12], we can see that the minimal time resolution is recorded in seconds. This is because the runners who are usually at the top of the rankings have a significant gap in finishing time between each other, so the timing systems with a resolution in seconds is accurate enough to meet the needs of marathons.

The current RFID timing system consists of an induction mat (consisting of multiple RFID readers) and a timing device for checkpoints. Depending on the width of the runner's track, a checkpoint may need several mats to cover the whole track. Because of this, setting up the checkpoints for a marathon is often very complicated and requires professional expertise to assist in the installation and ensure that it is functioning properly. Therefore, the hardware and labor costs are raised.

Study [1] analyzed the sources of timing errors in RFID-based timing systems and examined how different types of RFID tags can affect accuracy. Study [2] discussed how different RFID tag types use RFID timing systems in different sports and how they can affect the performance of the system. Also, the results of the experiment revealed that speed and the degree of tag overlap among several runners will affect the timing accuracy of the RFID timing system reading. Study [3] attempted to solve the problem of multiple RFID signal collisions by integrating different technologies, but it also significantly increased the cost of the system. The development of RFID timing systems still faces the challenge of high prices, as an induction mat contains multiple RFID readers. Meanwhile, to prevent the RFID reader in the mat from being damaged, a protective shield needs to be added to the mat, which makes it difficult to reduce its size and weight. These factors make it hard to reduce the complexity and cost of deploying an RFID-based timing system. Also, the mats may miss runners who do not pass right above the mat. To overcome missed detection, more RFID mats may be required and will further increase the cost.

BLE technology [14] has emerged as a viable alternative to RFID for timing and is particularly useful for smaller marathon events on a budget. BLE systems are scalable and can cover the entire marathon route with multiple timing points. They also have a number of advantages, including low power consumption, low cost, and small size, etc. Study [4] proposed a BLE timing system architecture. The runner wears a BLE tag that broadcasts BLE advertisements periodically and can be received by the specially designed sensor mat, which consists of several BLE receivers. Intuitively, due to the nature of BLE's short wireless communication range, typically less than ten m, the BLE receiver's reception of the broadcast advertisements from the runner's tag infers that they are physically near the BLE receiver, and the time is recorded. In this study, the authors analyzed the impact of different scenarios and timing errors. Study [5] proposed a low-cost BLE timing system based on the fact that the received signal strength (RSS) of the BLE signal will vary with the distance of the runner from the checkpoint. The closer to the checkpoint, the stronger the RSS will be. According to the study, the RSS will reach its "peak" point about 50 to 100 cm before the runner approaches the checkpoint. The authors claimed based on this observation that the mean time error is less than 100 ms, using a single mat (consisting of three BLE receiver). In this study, three mats were placed at a distance of 1 m (three sensor mats, with nine BLE receivers in total) to increase the reception rate, and the experiments revealed a detection rate of 99.86%. This study uses duplicate BLE receivers not only to overlap and enhance the detection rate but also to increase its hardware and deployment cost. As this type of system is based on receiving the BLE advertisement from the tag and using its RSS to determine the runner's time, one may maliciously emit a BLE signal from a remote location to mimic a runner passing the checkpoint. This is an important concern to BLE-based solutions in real marathons; this design does not have anti-cheating features and may be prone to disputes. In summary, RFID-based systems have been widely used in marathon events to provide automatic runner timing, but have been prohibitive in terms of their high hardware cost and high deployment complexity. BLE-based systems also have

been discussed in several prior studies to provide an alternative solution for small-scale marathons. However, the accuracy, reliability, and credibility of BLE-based systems is still unclear. To respond to the desperate need of a low cost, easy to deploy, reliable, and anti-cheating timing solution, this study proposed a new BLE timing system using multiple directional antennas to receive more characteristics of BLE advertisement broadcasted from the runner's BLE tag. This study is expected to achieve the following objectives:

- The proposed system can automatically time the marathon runners without human intervention and provide sufficient accuracy.
- The system is low cost, easy to deploy, and flexible compared with the conventional runner's timing solution.
- The system can accommodate different kinds of environments while maintaining time accurately.
- The system can detect cheating behaviors, such as taking detours and shortcuts.

III. System Architecture and Design

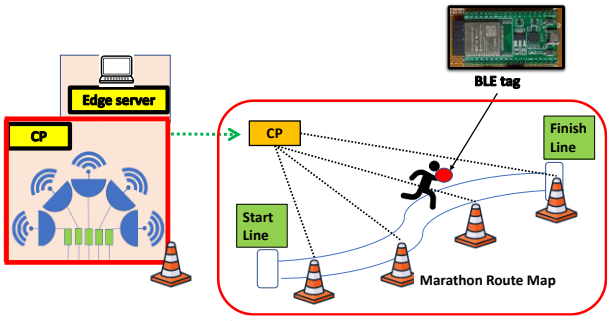

Fig. 2 The architecture of the proposed BLE-based multidirectional antenna timing system.

Fig. 2 shows the architecture of the proposed system. The runner in this system wears a BLE tag that will continuously broadcast BLE advertisements in 10 Hz. Several specially designed checkpoints (hereafter called CP) were installed along the marathon route, including at the start line and the finish line. A CP consists of several BLE receivers with different directional antennas; this design is aimed at receiving the wireless signal, or BLE advertisements, from the BLE tag worn on the runner to indicate that they passed by the CP. In contrast to the previous BLE timing system, the proposed CP design features the ability to collect BLE beacons using different directional antennas, which are aimed in different directions. As a directional antenna receives greater radio wave power in specific directions (in contrast to omnidirectional antennas that receive from a wide angle), our design allows us to collect more, different characteristics of RSS of the same BLE advertising packet or advertisement from a BLE tag moving along CPs. The details follow.

Fig. 2 shows three components of the system: the BLE tag, the CP, and the edge server inside the CP.

3.1 BLE Tag

A BLE tag worn by a runner is made by an ESP32-WROOM-32D [6] (hereafter ESP32), which is programmed to broadcast BLE advertisements in 10 Hz. The ESP32 output power level is 9 dBm with its 3.7 dBi internal antenna. The runner can wear the BLE tag as a wristband or headband. Compared to other BLE timing systems, which use the mat to receive BLE advertisements, suggesting that wearing the BLE tag on the shoe, our system removes this limitation and will not affect the performance significantly. Each BLE advertisement will contain the tag's ID to confirm the source of the packet by the receiver.

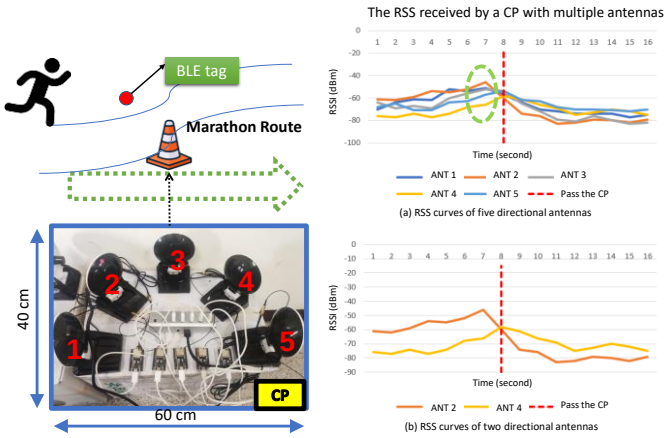

Fig. 3 A picture of a real CP and received RSS curves.

3.2 CP and Edge Server:

As shown in Fig. 3, a CP consists of five BLE receivers based on five ESP32, and each ESP32 is equipped with a 10 dBi gain 2.4 GHz directional antenna [10] aimed in different directions. The size of the CP is 40 cm x 60 cm. For CP's microprocessor selection, the following factors must be considered. First, it should be able to receive BLE advertisements without adding external components (i.e. another RF transceiver). Second, it should be able to have enough internal memory to buffer received BLE advertisements before reporting to the edge server. Third, it should provide an external communication interface to transmit the collected data to the edge server, and USB is a good choice to meet this requirement. With these factors in mind, we chose the ESP32 since we had the development kit on hand.

When a BLE tag broadcasts the advertising packet, the five BLE receivers indeed receive the same packet, but possibly with different RSS levels, due to the fact that it is received from different directional antennas with different polarization directions. This characteristic is novel compared to previous designs using multiple BLE receivers, which do not intend to receive RSS from the same wireless packet, and therefore, are not able to realize the proposed approach. As the RSS values from five ESP32s are measured, the data are transferred to the edge server via USB for further analysis.

The CP in this system can be designed in the form of a **traffic cone** next to the road and installed at key locations on the running path, allowing runners to run past it. The advantages of this design are that compared to traditional RFID mats or BLE mats that must be laid on the ground, our design has the advantages of easy and simple installation, lower labor costs,

and lower hardware equipment costs. Because it is not like a RFID or BLE mat that will be placed on the ground and trampled by runners, it also reduces the chance of equipment damage. Traditional mats must have a hard shell, which leads to increased costs, heavy shell weight, and troublesome installation.

Fig. 3 shows a photo of a real CP and how the proposed system works. The CP in this design has five directional antennas arranged in a half-moon shape installed on a shelf 46 cm high, each facing a different direction. The polarization directions of ANT1, ANT2, ANT3, ANT4, and ANT5 correspond to 180°, 135°, 90°, 45°, and 0°, respectively, in the polar coordinate system. Fig. 3(a) and (b) present the RSS curves from different antennas as the runner moves from left (close to the start line) to right (close to the finish line), passing the CP. Fig. 3(a) shows that the peaks (refer to the green dotted circle in the figure) of all RSS curves are in a short period of time before passing the CP; this finding is the same as that of the paper [5]. However, it is quite unreliable to use the peak of the RSS curve to infer that the runner has actually passed this place due to the fact that the RSS is often noisy. This demonstrates the need for our new approach to deal with this situation. In Fig. 3(a), we can see that all RSS curves intersect at the moment the runner passes the CP (indicated by the red dotted line), and this characteristic can be used to imply that the runner has passed the CP.

For a simplified view, Fig. 3(b) shows only ANT2 and ANT4; the polarization directions of these direction antennas correspond to 135° and 45°, respectively. As the runner begins to move from left to right before passing the CP, the RSS of ANT2 gradually raises until it is close to the point passing through the CP, and then the RSS begins to reflect and decrease gradually. We can see a similar RSS fluctuation from ANT4. When the runner is to the left of the CP, the RSS of ANT2 will always be larger than the RSS of ANT4, due to their different antenna polarization directions. Similarly, the RSS of ANT4 will always be larger than that of of ANT2 when the runner is to the right of the CP. The main reason is that the polarization directions of these two directional antennas are symmetrical, that is, the directions of the two antennas' amplified signals are symmetrical. When the tag moves to just passing the CP, the signal amplification of these two antennas at this location will be relatively small, so this characteristic occurs.

The above observations show us that the absolute value of RSS is less helpful, as it may be affected by many factors, but the difference among RSS curves (sourced from the same BLE advertisement) from multiple directional antennas is meaningful and can be used to detect that the runner has indeed passed by the CP. This is the basic idea of the proposed BLE design. The details are introduced below.

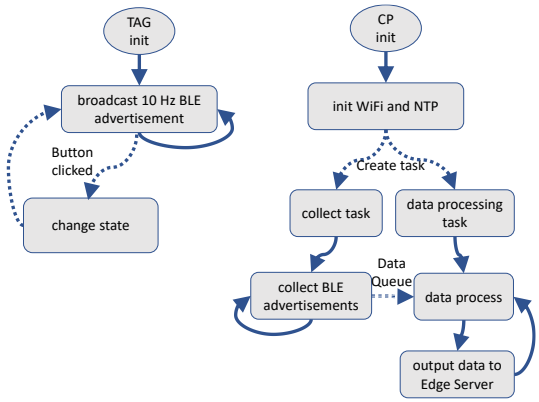

Fig. 4 The working flowcharts of the tag and the CP.

The working flow charts of the tag and CP are shown in Fig. 4. After the tag is powered on, it starts to broadcast BLE advertisements in 10 Hz frequency. In order to simplify the subsequent experimental procedures, a button on the tag was added so that runners can press the button when passing the CP. This will mark what time it is and change the internal state of the tag and the advertisement content (so we can mark the dotted red line based on it in Fig. 3[a] and Fig. 3[b]). When the CP receives its BLE broadcast packet, it can also know the tag's button has been pressed. These data can be used as ground truth for subsequent data analysis. Please note that the button only needs to be used to generate training data initially. When this system is actually used, the runner does not need to press this button.

After the CP is powered on, the Wi-Fi communication interface and network time protocol (NTP) will be initialized to obtain the current time. After that, two tasks will be created. The first task is continuously collecting BLE advertisements from tags and forwarding them to the data processing task for data preprocessing through the data queue and the collected data was processed in 1 sec unit and sent to the edge server through a USB for later analysis of the runner's behaviors.

An **edge server** is a computer that receives data from the five ESP32s by USB. A laptop computer was used in this prototype to collect data and run the deep learning algorithm and determine the runner's behavior and time, (i.e., that runner 1 is passing by CP 1). This can be replaced by an embedded system to miniature the size and lower the power consumption.

3.3 Preliminary Experiment

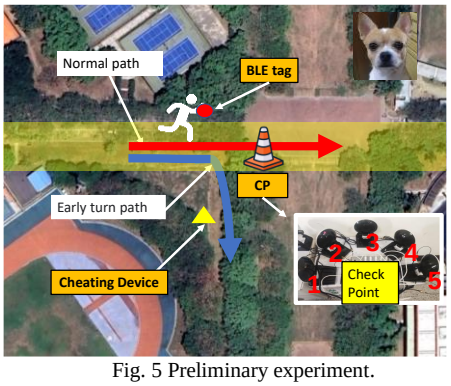

Fig. 5 Preliminary experiment.

Preliminary experiments were conducted to verify our idea. As shown in Fig. 5, a runner with a BLE tag ran on the path

from left to right, following the yellow route. A normal runner should follow the "normal path" (refer to the red arrow) in the figure and pass by the CP (at a distance range of 1 to 10 m). However, a cheating runner may take a shortcut (refer to the blue arrow) by turning early and not following the route. Alternatively, a cheating runner might use a cheating device to try and generate the BLE signals to mimic a normal runner passing the CP.

3.3.1 Time Resolution of RSS

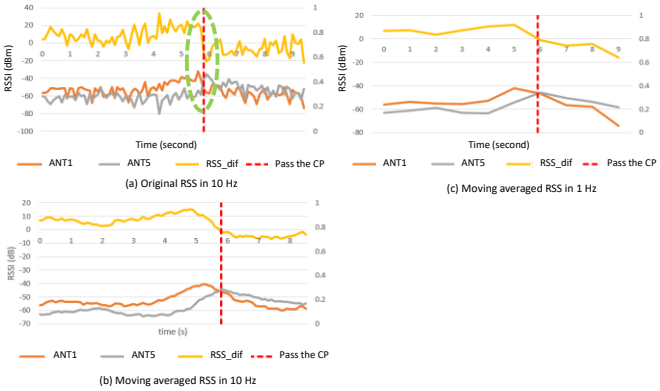

Fig. 6 The RSS received by the CP with multiple antennas, generated by a runner running on the normal path.

Fig. 6 shows the RSS from an experiment with a runner running on the normal path (red arrow in Fig. 5) from left to right. In order to simply the explanation, Fig. 6(a) only shows the RSS collected by the CP (refer to the CP in Fig. 5) from ANT1 and ANT5 (which are pointed to 180° and 0°, respectively). The *RSS_dif* curve in the figure indicates the difference between ANT1 and ANT5. The RSS in Fig. 6(a) is collected by the CP at a frequency of 10 Hz. Although the RSS curve of ANT1 and ANT5 are noisy, we can still see that RSS_dif drops to zero at the intersection (refer to the green dotted circle in Fig. 6[a]) of the two RSS curves. In addition, the runner is passing the CP at this point. We perform 1 sec moving average processing on the RSS of Fig. 6(a) and obtain the Fig. 6(b) with a relatively smooth RSS. We find that the characteristics previously discovered in Fig. 6(a) are more obvious in Fig. 6(b), where RSS_dif drops to zero, indicating the runner passing the CP. In order to reduce the amount of data processed by the subsequent edge server, the time resolution of our RSS is reduced to a frequency of 1 Hz. In this case, the previously discovered characteristics are still clearly present, with RSS_dif decreasing to 0 close to where the runner passes the CP. Based on this result, in subsequent experiments, we will set the CP to collect RSS data at 1 Hz for subsequent data analysis.

3.3.2 RSS of Normal and Cheating Runners or Devices

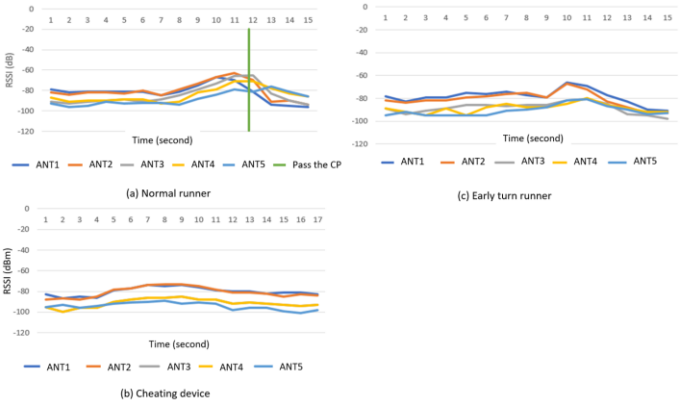

Fig. 7 The RSS from normal runner and cheating runner scenarios.

We conducted the following experiments to verify our proposed approach to discriminate between normal runner and cheating behaviors. We selected two cheating scenarios, including cheating runners who turn early and take shortcuts and cheating runners who use a cheating device to generate normal runner signals. The RSS received by the CP is shown in Fig. 7.

Since our BLE-based running timing system uses the RSS change of the BLE tag received by the CP to determine whether the runner actually ran past the CP, the purpose of this experiment is to ask whether, in the case there is a malicious BLE tag installed near the CP (refer to the yellow triangle in Fig. 5) and it can broadcast BLE advertisement signals at different power levels (i.e., from weak to strong, and to weak) to emulate a normal runner's RSS, can it effectively deceive the CP into pretending that a runner is passing by? Fig. 7(b) shows the RSS generated by the cheating device, although it tries to emulate RSS changes, it is difficult to generate the characteristics of a normal runner's RSS and make the CP's RSS curves of two specific antenna have a crossover. Therefore, it can be seen that the RSS curve in Fig. 7(b) is not the same as the normal runner RSS in Fig. 7(a). Similarly, the RSS shown in Fig. 7(c) for the runners who turn early and take shortcuts obviously does not have the same characteristics as the RSS of normal runners. In the later experiment, we use deep learning algorithms to show that it can be discriminated in high accuracy. The details follow.

3.3.2 Packet Reception Ratio

In the proposed system, multiple runners will carry their own BLE tags and pass the CP at the same time. This will allow us to determine whether the transmission data will be lost due to packet collision due to multiple BLE tags broadcasting BLE advertisements at the same time. In the following experiment, multiple runners were asked to carry different numbers of BLE tags, from 1 to 20, and run past the CP to see if different numbers of BLE tags will lower the packet reception ratio (PRR) received by the CP. Please note that the calculation here is based on the BLE tags broadcast advertisement in 10 Hz, and the CP can completely receive these packets. We conducted the same experiments in indoor and outdoor environments. However, in our experiments, whether indoors or outdoors, there is no consistent impact on PRR. Even if there is only one BLE tag, the PRR will not be 100% in our environment due to a variety of radio equipment working in the area. The range of PRR

fluctuates between 79% and 87%. This result shows that the number of BLE tags does not have a significant impact on the PRR of the CP, due to the fact that BLE has some random mechanism to broadcast packets on three different BLE channels: 37, 38, and 39. In subsequent data analysis, the lost packet information will be compensated for by linear interpolation. As the example shown in Fig. 9, in this case, the packet in 2nd second is lost, only the packets in the first and third second are received. Assuming that the runner's running direction and speed remain unchanged, the RSSI of the lost packet in 2nd second can be approximated with linear interpolation by these two known values, and can still maintain correct detection that the runner passed through the CP.

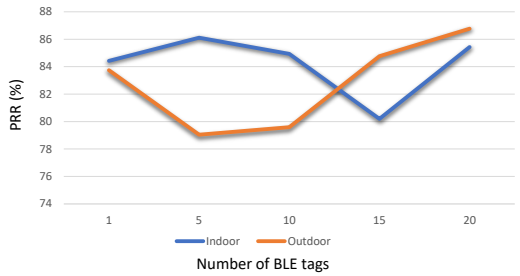

Fig. 8 PRR of the CP vs. number of BLE tags.

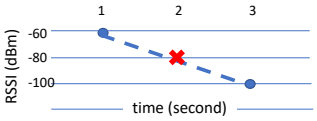

Fig. 9 The linear interpolation of the lost packet.

3.4 Full-Scale Experiment

As in the previous section, the preliminary experiment verified that our idea to build a BLE-based timing system is feasible. In this section, we further expand the scale of the experiment to verify the proposed system. The goals of this experiment are to evaluate different deep learning algorithms and their accuracy in different parameter sizes and training sets. The full-scale experiment was conducted in our university campus. We collected runners' RSS in the following four locations:

L1: The driveway at the entrance of the building
L2: The corridor inside the building
L3: The sidewalk next to the building
L4: The driveway next to the sports field (where the preliminary experiment was conducted)

These locations will be referred to below as L1, L2, L3, and L4. The equipment settings of the above experimental locations are the same to the ones in Fig. 5. The runner runs across the CP at a distance of 1 to 10 m; the runner's running direction is from ANT1 to ANT5 of the CP. Twenty runners participated in the experiments and collected 120 RSS logs among these four locations.

3.4.1 Deep Learning Algorithms

After the CP received RSS from BLE tags, the data was then forwarded to the edge server and used deep learning algorithms to determine the runners' behaviors. We evaluated the deep neural network (DNN) and long short-term memory (LSTM) at two parameter sizes of about 1,000 (hereafter called "the small model") and about 13,000 (hereafter called "the big model"). In this system, simpler algorithms and parameter sizes must be considered, since we may implement deep learning algorithms in memory-constrained embedded systems, such as the ESP32 we use in CP. Therefore, the selection of deep learning models with different parameter sizes is an important topic and will be discussed below.

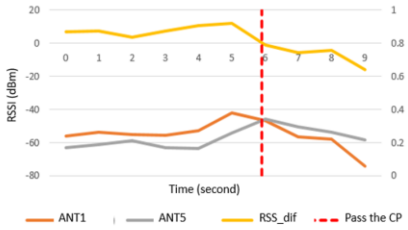

Time (second)	0	1	2	3	4	5	6	7	8	9
Ground truth	0	0	0	0	0	0	1	1	1	1
Correct detection	0	0	0	0	0	0	1	1	1	1
Correct detection with an error of 1 second	0	0	0	0	0	1	1	1	1	1
Correct detection with an error of 2 second	0	0	0	0	0	0	0	0	1	1
Incorrect detection	0	0	0	0	0	0	1	1	0	1

Fig. 10 Ground truth and the algorithm output explanation.

We use Fig. 10 to illustrate the working mechanism of our deep learning algorithm. The runner will press the button on their BLE tag to record the exact time they pass the CP during their run. We establish ground truth based on the above method (refer to the table in the above figure). "0" indicates that the runner has not yet passed the CP, and "1" indicates that the runner has passed the CP. The 0 and 1 in the "ground truth" row represent the real runner status. In our system, the deep learning algorithm will input the current RSS of multiple directional antennas and use it to determine and output whether at this moment, the runner "has" or "has not yet" passed through the CP. Therefore, in the "correct detection" row, the algorithm accurately outputs the same runner status as the ground truth, which means that the algorithm's decision is exactly the same as the actual behavior and is 100% correct.

In the row "Correct detection with an error of 1 sec," it is shown that the algorithm determines that the runner passed the CP 1 sec earlier (please refer to the green dotted circle); in this case, the system correctly determined that the runner had passed, but the time recorded for passing had an error of 1 sec. The row "correct detection with an error of 2 sec" shows that the algorithm determined that the runner passed the CP two seconds late (refer to the blue dotted circle); in this case, the system correctly determined that the runner passed the CP, but the recorded time is off by 2 sec.

The "incorrect detection" row shows that the algorithm first

determines that the runner has passed the CP, but then suddenly determines that they have "not passed the CP" for 1 sec (refer to the red dotted circle), and then subsequently judges that they have "passed the CP." Although the algorithm outputs most of the runner's states correctly, there are still 1 sec errors.

Based on this explanation, in the following, we use DNN and LSTM (refer to Fig. 11) to predict the runner's state. In DNN, the input data to the model is the RSS values of five directional antennas in 1 sec, and the output is whether the runner's status has passed CP (0 or 1). In LSTM, the input data to the model are the RSS values of five directional antennas in 3 sec, and the output is whether the runner's status has passed CP (0 or 1).

DNN

Small model

Layer (type)	Output Shape	Param #
input_22 (InputLayer)	[(None, 5)]	0
dense_84 (Dense)	(None, 32)	192
dropout_59 (Dropout)	(None, 32)	0
dense_85 (Dense)	(None, 16)	528
dropout_60 (Dropout)	(None, 16)	0
dense_86 (Dense)	(None, 16)	272
dropout_61 (Dropout)	(None, 16)	0
dense_87 (Dense)	(None, 1)	17

Total params: 1,009
Trainable params: 1,009
Non-trainable params: 0

Big model

Layer (type)	Output Shape	Param #
input_2 (InputLayer)	[(None, 5)]	0
dense_4 (Dense)	(None, 32)	192
dropout_3 (Dropout)	(None, 32)	0
dense_5 (Dense)	(None, 64)	2112
dropout_4 (Dropout)	(None, 64)	0
dense_6 (Dense)	(None, 128)	8320
dropout_5 (Dropout)	(None, 128)	0
dense_7 (Dense)	(None, 16)	2064
dense_8 (Dense)	(None, 1)	17

Total params: 12,705
Trainable params: 12,705
Non-trainable params: 0

LSTM

Small model

Layer (type)	Output Shape	Param #
input_36 (InputLayer)	[(None, None, 5)]	0
lstm_68 (LSTM)	(None, None, 8)	448
dropout_66 (Dropout)	(None, None, 8)	0
lstm_69 (LSTM)	(None, 8)	544
dropout_67 (Dropout)	(None, 8)	0
dense_35 (Dense)	(None, 1)	9

Total params: 1,001
Trainable params: 1,001
Non-trainable params: 0

Big model

Layer (type)	Output Shape	Param #
input_3 (InputLayer)	[(None, None, 5)]	0
lstm_4 (LSTM)	(None, None, 32)	4864
dropout_4 (Dropout)	(None, None, 32)	0
lstm_5 (LSTM)	(None, 32)	8320
dropout_5 (Dropout)	(None, 32)	0
dense_2 (Dense)	(None, 1)	33

Total params: 13,217
Trainable params: 13,217
Non-trainable params: 0

Fig. 11 The DNN and LSTM architectures used in our experiment.

3.4.2 Analysis Results

training set		val set	test set	training acc	val acc	test acc	correct detection with timing error (sec)	incorrect detection (sec)		training acc	val acc	test acc	correct detect with timing error (sec)	incorrect detection (sec)
L1	L3	L2	L4	96.43%	97.67%	96.30%	3	0		96.95%	94.00%	98.59%	1	0
		L4	L2	97.62%	100.00%	98.21%	0	1		95.43%	90.14%	82.00%	7	2
L1	L2	L3	L4	98.62%	94.59%	97.53%	2	0		97.62%	94.94%	98.59%	1	0
		L4	L3	99.31%	97.30%	98.82%	1	0		97.02%	91.55%	98.73%	1	0
L1	L4	L3	L2	95.76%	100.00%	100.00%	0	0		95.77%	98.73%	80.00%	9	1
		L2	L3	98.18%	100.00%	98.82%	1	0		95.77%	96.00%	97.47%	1	1
L3	L2	L1	L4	100.00%	100.00%	95.06%	1	3		95.35%	94.92%	94.37%	4	0
		L4	L1	100.00%	100.00%	96.83%	2	2		91.47%	88.73%	93.22%	2	6
L3	L4	L1	L2	99.24%	97.06%	100.00%	0	0		96.67%	92.37%	72.00%	9	5
		L2	L1	100.00%	100.00%	95.24%	2	3		95.33%	78.00%	94.92%	5	1
L2	L4	L1	L3	99.08%	100.00%	98.82%	1	0		95.87%	98.31%	97.47%	2	0
		L3	L1	100.00%	96.43%	95.24%	2	4		95.87%	94.94%	98.31%	1	1
DNN (small model) AVERAGE				98.69%	98.59%	97.57%	15	13	LSTM (small model) AVERAGE	95.76%	92.72%	92.14%	43	17

Fig. 12 The performance of DNN and LSTM (small models).

In the evaluation, in all analytic combinations, we select the RSS data from two locations as a training set, and select RSS data from one location each for the validation set and the test set. For example, referring to Fig. 12, the first test combination in small model DNN used L1 and L3 for the training set, L2 for the validation set, and L4 for the test set. In this figure, the average training accuracy, validation accuracy, and test accuracy of the small model DNN are 98.69%, 98.59%, and 97.57% respectively, and 13÷(13+15) = 46% is the "correct detection with timing error."

Please note that the unit for "correct detection with timing error" and "incorrect detection" is second, as in our design the model will output a prediction every second. For small model LSTM, the average training accuracy, validation accuracy, and test accuracy are 95.76%, 92.72%, and 92.14%, respectively, and 17÷(17+43) = 28% is the error in detecting whether the runner has passed. Comparing the two, DNN has good results when the number of parameters is small, and overall it beats the LSTM.

training set		val set	test set	training acc	val acc	test acc	correct detection with timing error (sec)	incorrect detection (sec)		training acc	val acc	test acc	correct detection with timing error (sec)	incorrect detection (sec)
L1	L3	L2	L4	97.62%	97.67%	96.30%	3	0		95.43%	100.00%	98.59%	1	0
		L4	L2	97.62%	97.67%	98.21%	0	1		95.94%	90.14%	98.00%	1	0
L1	L2	L3	L4	94.48%	97.30%	95.06%	4	0		92.26%	94.94%	95.77%	3	0
		L4	L3	97.24%	97.30%	98.82%	1	0		95.24%	90.14%	98.73%	1	0
L1	L4	L3	L2	98.18%	100.00%	100.00%	0	0		94.71%	94.94%	96.00%	2	0
		L2	L3	98.18%	95.24%	100.00%	0	0		96.83%	92.00%	96.20%	3	0
L3	L2	L1	L4	98.21%	100.00%	93.83%	1	4		95.35%	94.92%	92.96%	5	0
		L4	L1	99.11%	100.00%	97.62%	2	1		91.47%	90.14%	99.15%	1	0
L3	L4	L1	L2	96.97%	97.06%	100.00%	0	0		93.33%	96.61%	98.00%	1	0
		L2	L1	98.48%	100.00%	92.86%	2	7		92.67%	98.00%	99.15%	1	0
L2	L4	L1	L3	99.08%	100.00%	98.82%	1	0		90.08%	96.61%	98.73%	1	0
		L3	L1	96.33%	100.00%	94.44%	2	5		95.04%	97.47%	97.46%	3	0
DNN (big model) AVERAGE				97.63%	98.52%	97.16%	16	18	LSTM (big model) AVERAGE	94.03%	94.66%	97.40%	23	0

Fig. 13 The performance of DNN and LSTM (big models)

Referring to Fig. 12, the training accuracy, validation accuracy, and test accuracy of the big model DNN is very similar to the small model DNN. However, for the big model LSTM, the average test accuracy is raised from 92.14% to 97.4% compared to the small model LSTM. Meanwhile, "incorrect detection" for big model LTSM is 0%. This is an important advantage because we know that "incorrect detection" is not acceptable for the runner timing system (i.e., especially from the aspect of providing anti-cheating features) and should be avoided at all costs. For "correct detection with timing error," after investigation, we found that all timing errors are less than 1 sec.

The parameter size of the DNN has less impact on the accuracy, and although both DNN models do not perform very well in the L1 and L4 cases, they still have an accuracy of over 92.86%. The reason may simply be that the L1 and L2 environments are relatively wide and the distance between the runner and the CP is relatively long, resulting in less significant RSS changes when running by the CP. DNNs are less able to cope with such insignificant RSS changes, resulting in slightly lower accuracy.

For small model LSTM, the worst test accuracy for L2 only reaches 72%, which is an unacceptable level. This might be due to the fact that LSTM is more affected by the temporal relationship between sequence data and that too much RSS noise leads to noisy RSS data, resulting in bad accuracy. However, for the LSTM of large models, the test accuracy improves significantly. The minimum test accuracy increases to 92.96% when using L4 as the test set. This evaluation shows that the LSTM with a big model is a good candidate for this application and will be applied in the following analysis. The parameter size of the big model LSTM is 13,217, and if each parameter is a 4-byte floating-point variable, the model requires about 13,217 x 4 = 52,868 bytes of memory space, or about 53 kBs. This memory requirement is acceptable in embedded systems and further supports the portability of our design to memory-constrained architectures.

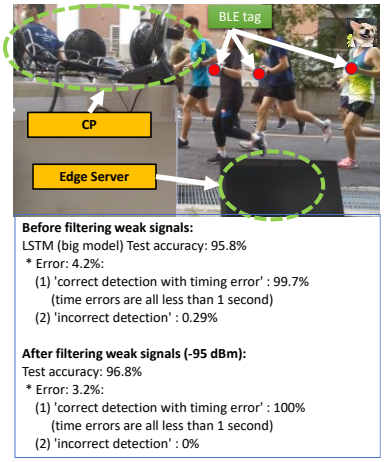

Fig. 14 Additional 20-runner experiment and analysis of the result.

In order to further understand the performance of this system, we once again invited 20 runners to conduct experiments in the driveway at the entrance to the Innovation Building (L1). We collected the RSS data of these runners for analysis to see whether the performance of the LSTM system is accurate. At the same time, we set up the high-speed camera to record ground truths and confirmed that the time of running through CP was close to the ground truth from the BLE tags. In the end, only 19 people actually participated in the experiment, due to a faulty BLE tag device. Among the 19 runners who participated in the run, 14 were sports majors and 5 were non-sports majors. The collected data was used as test set to the big model LSTM with the RSS from all the previous experiments (L1, L2, L3 and L4) as the training set.

The analytic result showed the average test accuracy was 95.8%. Of the remaining 4.2% error cases, 99.71% were "correct detection with timing error," and all the timing errors were less than 1 sec. Only 0.29% is "incorrect detection" in this experiment. An in-depth analysis of the reason for this 0.29% error shows that in some cases, the signal generated by distant runners is very weak (i.e., less than -95 dBm) and is susceptible to interference, resulting in an RSS curve that has characteristics similar to when passing by CP. Therefore, we filtered out excessively weak signals in the data preprocessing stage and removed all signals with an RSS less than -95 dBm. As a result, we found that the test accuracy could be improved to 96.8%, and the remaining 3.2% were "correct detection with timing error," and the time errors were all less than 1 sec. If we can relax the time accuracy requirement to plus or minus 1 sec, the test accuracy of this system will become 100%, which is completely correct. In fact, our system meets the needs of marathon races, as seconds are used as the smallest unit for marathon recording.

IV. Conclusion and Future Works

This paper proposes a marathon runner timing system based on BLE with multidirectional antenna architecture. Compared with previous related research, this design has the advantages of high accuracy and resistance to environmental changes. We conducted experiments in four different locations to collect data and used deep learning algorithms to determine runner's behaviors. DNN and LTSM with different parameter sizes were evaluated, and the results show that the big model LTSM is suitable for our application, and this model can be ported to a memory-constrained embedded system as it only needs about 53 kBs for the model parameters. In order to further confirm the stability and accuracy of our system, we conducted another experiment with 20 runners passing by the CP at the same time. The results indicate, after adding a threshold to filter weak RSS in CP, the accuracy of correctly determining "passing by" behavior can reach 100%, and the passing time error is plus or minus 1 sec. Since the current timing of general marathon events is based on seconds as the smallest unit, the timing accuracy provided by this system is sufficient for use in marathons. For higher accuracy requirements, traditional high-speed cameras still must be used to determine final timing and sequence.

At the same time, in this study, we only briefly used two commonly used deep learning algorithms to demonstrate the feasibility of our timing system and show that it is small enough to run on an embedded system. Subsequent research can further optimize the algorithms to see if the accuracy and timing error can be further improved.

CPs are not placed on the ground like the RFID or BLE mats used in the previous studies. As our CP is relatively lightweight and easy to install, like a traffic cone, this creates the incentive for use in real marathon events. In addition, in the current design, the CP's edge server is run using a laptop computer, which executes a deep learning algorithm to analyze the runner's behavior. In the future, we can use embedded systems or even MCU-level systems instead of ESP32 to design the edge server, so that we can further reduce the power consumption, physical size, and hardware cost of the system.

Meanwhile, in our implementation, the runner status output by edge server is shown on the screen. In the future, in the actual sports system, this information can be sent to the remote server through mobile networks such as 4G/5G, so that the audience and sports coaches can view the information in real time. Having the real-time status of all runners will make the marathon more interesting and credible.

In this study, the main reason for reducing the 10 Hz RSS to 1 Hz is to lower the amount of data in the CP's buffer (using an ESP32 microprocessor), after which the data in the buffer is sent to the edge server for computation. Another reason is that marathon races only require timing to be accurate to a matter of seconds. To meet this requirement, this study used the smallest unit of seconds in designing the system. If necessary, this system can also be used to design the system directly with 10 Hz RSS.

In our experiments, we currently use five directional antennas to judge runners' behavior. In the future, we may be able to consider different placements and arrangements of directional antennas or use different numbers of directional antennas to see if it will affect the final accuracy. Also, currently we use discrete directional antennas to collect RSS. In the future, we may consider designing a printed circuit board antenna to integrate multiple directional antennas on one circuit board and further reduce costs and the space.

Regarding comparing the proposed system to related timing systems, RFID is the most commonly used method in actual marathons. Nevertheless, even disregarding equipment and installation costs, missed detection is still possible under some circumstances. Furthermore, conventional BLE-based timing systems suffer from an inability to determine malicious behaviors, not to mention having similar problems to RFID-based systems. Among the marathon timing systems, there is no doubt that the most accurate are optical methods, that is, high-speed cameras, for measuring when runners pass the station (assuming high equipment and labor costs are not a concern). Therefore, in our study, we use the camera as the ground truth to compare and validate our system in the final experiment and show that our design is viable. In short, it may not be reasonable to compare different marathon timing techniques without considering their limitations.

In summary, this study opens up a new direction, using multiple directional antennas to collect wireless signal RSS to determine the behavior of marathon runners. This study designed the system and conducted experiments to verify that the ideas we proposed are correct and feasible. In the future, we hope to further improve and optimize the abovementioned issues of this system, and use this system in real-world marathons.

ACKNOWLEDGEMENTS

This work was financially/partially supported by the Advanced Institute of Manufacturing with High-tech Innovations (AIM-HI) from The Featured Areas Research Center Program within the framework of the Higher Education Sprout Project by the Ministry of Education (MOE) in Taiwan. The authors would like to thank Pei-Jyi Lee and Pin-Chen Kuo for their excellent assistance.

REFERENCES

[1] James Johnston, "Work in Progress: RFID Sports Timing System", Southern Scholars Honors Program Senior Project Proposal Information Sheet, [online] Available: https://knowledge.e.southern.edu/senior research/23.

[2] Kolaja and J. Ehlerova, "Effectivity of Sports Timing RFID System, Field Study," Sep. 2019, doi: https://doi.org/10.1109/rfid-ta.2019.8892108.

[3] R. Alesii, P. D. Marco, F. Santucci, P. Savazzi, R. Valentini, and A. Vizziello, "Backscattering UWB/UHF hybrid solutions for multi-reader multi-tag passive RFID systems," EURASIP Journal on Embedded Systems, vol. 2016, no. 1, May 2016, doi: https://doi.org/10.1186/s13639-016-0031-0.

[4] C.-I. Sun, J.-T. Huang, S.-C. Weng, and M.-F. Chien, "City Marathon Active Timing System Using Bluetooth Low Energy Technology," Electronics, vol. 8, no. 2, p. 252, Feb. 2019, doi: https://doi.org/10.3390/electronics8020252.

[5] D. Perez-Diaz-de-Cerio, Á. Hernández-Solana, A. Valdovinos, and J. Valenzuela, "A Low-Cost Tracking System for Running Race Applications Based on Bluetooth Low Energy Technology," Sensors, vol. 18, no. 3, p. 922, Mar. 2018, doi: https://doi.org/10.3390/s18030922.

[6] B. Shin, J. H. Lee, C. Yu, H. Kyung and T. Lee, "Received Signal Strength-Based Robust Positioning System in Corridor Environment," in IEEE Transactions on Instrumentation and Measurement, vol. 71, pp. 1-15, 2022, Art no. 8504215, doi: 10.1109/TIM.2022.3190522.

[7] V. Bianchi, P. Ciampolini and I. De Munari, "RSSI-Based Indoor Localization and Identification for ZigBee Wireless Sensor Networks in Smart Homes," in IEEE Transactions on Instrumentation and Measurement, vol. 68, no. 2, pp. 566-575, Feb. 2019, doi: 10.1109/TIM.2018.2851675.

[8] H. -C. Lee and T. -T. Lin, "Low-Cost Indoor Human Tracking by Utilizing Fluctuation of Received Radio Signal Strength," in IEEE Sensors Journal, vol. 20, no. 21, pp. 13029-13036, 1 Nov.1, 2020, doi: 10.1109/JSEN.2020.3001055.

[9] "ESP32WROOM32D & ESP32WROOM32U Datasheet." Available: https://www.espressif.com/sites/default/files/documentation/esp32-wroom-32d_esp32-wroom-32u_datasheet_en.pdf

[10] "High Gain 2.4GHz WiFi Antenna 10dBi RP-SMA Male Wireless WLAN Directio," Shenzhen Faycent Technology Co.,Ltd. https://rfcablesantennas.com/products/high-gain-2-4ghz-wifi-antenna-10dbi-rp-sma-male-wireless-wlan-directional-radar-antenna-with-rg174-cable-1m-router (accessed Dec. 06, 2023).

[11] "World Athletics Home Page | World Athletics," worldathletics.org. https://worldathletics.org

[12] "TCS London Marathon 2023: Results," Mika timing. https://results.tcslondonmarathon.com/2023/?pid=list (accessed Dec. 04, 2023). ChampionChip Available: https://www.championchip.com.my/

[13] "EventResults," MYLAPS. https://www.mylaps.com/timing-solutions-active/eventresults/ (accessed Dec. 04, 2023).

[14] "Intro to Bluetooth Low Energy," *Bluetooth® Technology Website*, Mar. 26, 2017. https://www.bluetooth.com/bluetooth-resources/intro-to-bluetooth-low-energy/